Submitted to Nucl. Instrm. & Meth. in Phys. Research

LNF-91/025 (P)
21 Maggio 1991

S.Bartalucci, R.Boni, A.Gallo, M.Serio, R.Scalia, B.Spataro, G.Vignola, L. Palumbo:

A PERTURBATION METHOD FOR HOM TUNING IN A RF CAVITY

INFN - Laboratori Nazionali di Frascati
Servizio Documentazione

LNF-91/025 (P)
21 Maggio 1991

A PERTURBATION METHOD FOR HOM TUNING IN A RF CAVITY

S.Bartalucci, R.Boni, A.Gallo, M.Serio, R.Scalia, B.Spataro, G.Vignola
INFN - Laboratori Nazionali di Frascati , P.O.Box 13, I - 00044 Frascati (Roma), Italy

L. Palumbo
Dip. Energetica, Univ. La Sapienza, Via A. Scarpa 14, 00161 (Roma), Italy.
and Laboratori Nazionali di Frascati dell'INFN, I - 00044 Frascati (Roma), Italy

ABSTRACT

The cure of multibunch instabilities is of utmost importance for the next generation of very high current storage rings. The parasitic modes of the RF cavities are chiefly responsible of these instabilities. A perturbation method is proposed to decouple the cavity parasitic modes from the bunch relative oscillation sidebands,without affecting the fundamental mode. Signal level measurements on a test pill-box cavity give encouraging results.

1. - INTRODUCTION

Multibunch instabilities are among the most harmful problems in the design of high current storage rings lately proposed [1,2] and in particular of the high luminosity flavor factories such as DAΦNE [3]. Preliminary calculations, which are worked out with theoretical models, show that the instability growth rate at the nominal current can be far above the damping rate induced by radiation or by a powerful feedback system [3]. Therefore this problem deserves a careful analysis of both instability sources and cures.

The parasitic Higher Order Modes (HOMs) of the RF cavity are mostly responsible of such instabilities. In fact they induce coupling of the relative motion of N bunches through the e.m. fields left behind in the cavity by the bunches themselves. In the frequency domain the relative bunch motion shows a twofold comb-like line spectrum (sidebands) around the

harmonics of the revolution angular frequency ω_0, with stable and unstable sidebands for each relative mode. The instability growth rate depends on the location of these sidebands with respect to the HOM spectrum. Each HOM is described by a complex impedance $Z(\omega)$ with a resonant frequency ω_r, shunt impedance R and quality factor Q. The real part of the impedance causes the instability.

For large size accelerators (1÷10 km), the sidebands are spaced at 30÷300 kHz, so that many of them are coupled to the HOM real impedance. The usual method adopted to reduce the coupling to the HOMs consists in absorbing a significative part of the energy lost by the bunch thereby lowering the shunt impedance (and simultaneously the Q factor, the ratio R/Q being almost constant). So far the HOM damping is obtained by coupling the cavity to loop antennas or by using absorbing materials. More recently the use of waveguides has been proposed [4,5]. The effectiveness of such method is quite good if one can obtain a strong reduction of the Q factor such that the condition: $Q \ll \pi\omega_r/N\omega_0$ is satisfied. Otherwise one can be left with a residual growth rate that has to be counteracted by the radiation damping and by a feedback system. Moreover for those modes that have been only partially damped one can observe on one side the reduction in the growth rate of the coupled instabilities, on the other side the rise of new ones, formerly uncoupled.

A different approach to the problem may be proposed for small accelerators, starting from the consideration that ideal infinite-Q HOMs do not couple to the sidebands unless of a precise frequency overlapping. In fact in small ring accelerators (≈100 m) the sidebands are spaced at several of MHz and therefore they are more unlikely to couple to the HOMs. However we know that during the accelerator operation the HOM frequencies may drift making the coupling possible. In this case it would be certainly preferable to control the shift of the offending HOM.

In this paper we describe the preliminary theoretical and experimental results concerning the frequency shift control of parasitic modes in a pill box cavity. The frequency shift is caused by two perturbing metallic objects located at the cavity walls. Our aim is to find out general features of the HOMs with regard to the frequency shift related to the position and size of the perturbing objects. Two perturbing objects allow one to fulfill two conditions: a) to keep the frequency of the fundamental accelerating mode unchanged, b) to shift a single HOM by a given amount. However, in principle the method can be extended considering m perturbing objects and control the frequency of (m-1) HOMs.

2. - PERTURBATIVE METHOD

Two small metallic objects, with volume τ_1 and τ_2, located somewhere inside a RF cavity perturb "locally" the e.m. fields and lead to a frequency shift of all the eigenmodes such that the balance between the average energy stored in the electric and magnetic fields is restored. The relative frequency shift of a cavity eigenmode, whose unperturbed frequency is ω_0, is expressed by Slater's perturbation theorem [5]:

$$\frac{\omega - \omega_0}{\omega_0} = \frac{\int_{Volume} (\mu H^2 - \varepsilon E^2)\, d\tau}{U}$$

where the integral is performed on the volume of the perturbing objects and $U=2U_m=2U_e$ is the average stored energy (twice the electric or magnetic energy). The frequency shift depends

on the balance between the electric and magnetic energy "subtracted" by the conducting objects. Considering objects with simple shape and symmetry, one can relate the "subtracted energy" to the local unperturbed fields. For a single spherical object of volume "τ" we have:

$$\frac{\omega - \omega_0}{\omega_0} = \frac{\left(k_1 \mu H^2 - k_2 \varepsilon E^2\right)\tau}{U} \equiv \frac{k_1 U_m - k_2 U_e}{U} \qquad (1)$$

where U_m and U_e are the electric and magnetic energies stored in the unperturbed field inside the volume τ. The form factors k_1=1.5 and k_2= 3, as computed for a sphere in the approximation of uniform static fields [5], account for the total field distortion inside the object and in the vicinity of its surface.

To determine τ_1 and τ_2 we require that eqn. (1) gives zero frequency shift for the fundamental mode:

$$k_1 U_m - k_2 U_e = 0 \qquad (2)$$

and that the relative frequency shift of a particular cavity mode be δ:

$$\frac{k_1 U_m - k_2 U_e}{U} = \delta \qquad (3)$$

Once the amount of desired frequency shift δ is chosen, by combining eqs. (2) and (3) we get τ_1 and τ_2. Thus the tuning of a given mode is accomplished without affecting the fundamental frequency.

3. - PILL BOX HOMS. THEORETICAL AND EXPERIMENTAL RESULTS

In order to understand the effectiveness of the method we have analyzed the effect of two small metallic hemispheres on the HOMs of a pill box cavity whose fields expressions are well known. The relevant geometry is described in Fig.1. One object, whose volume is τ_1, is located on the outer cylindrical surface, while the other one, whose volume is τ_2, is located on one end of the pill-box and can be radially displaced. Our aim is to calculate the volumes τ_1 and τ_2 as function of the radial position r, such that the frequency shift requirements are fulfilled. We have computed the values of the inserted volumes as normalized to the cavity volume V and per unit of relative frequency shift $(\tau_1/V)/\delta$ and $(\tau_2/V)/\delta$ for several TM and TE modes. The two emispheres, being located at the pill box surface, because of the image theorem have the same form factor as a sphere.

Mode TM_{010} (fundamental mode)

Wherever we put the two objects, its frequency has to stay constant.This condition yields:

$$\frac{\tau_1}{\tau_2} = \frac{2J_0^2\left(\frac{x_{01} r}{a}\right) - J_1^2\left(\frac{x_{01} r}{a}\right)}{J_1^2(x_{01})}$$

Mode TM_{110}

This mode is degenerate in an ideal cavity, corresponding to two orthogonal directions of polarization of the electric field: $\phi = \pi/2$ and $\phi = 0$. Both are shifted with our mechanism. Condition on the HOM frequency shift for $\phi = \pi/2$ yields:

$$\frac{\tau_2}{V\,\delta} = \frac{\frac{1}{3} J_0^2(x_{11})\, J_1^2(x_{01})}{J_1^2(x_{11})\left[2J_0^2\left(\frac{x_{01} r}{a}\right) - J_1^2\left(\frac{x_{01} r}{a}\right)\right] + J_1^2(x_{01})\left[J_1^2\left(\frac{x_{11} r}{a}\right) - 2J_1^2\left(\frac{x_{11} r}{a}\right)\right]}$$

In Fig.2 we show the plots of (τ_1/V) and (τ_2/V) for δ=0.001 versus the "normalized" displacement r/a of the object τ_2. It is worth noting that there exists a region for r/a (between .6 and .7) where the two volumes are negative. This case, requiring the insertion of negative volumes, has no physical relevance for our pill box cavity case. Nevertheless, in general, one can "add" or "subtract" small volumes if the unperturbed frequencies are obtained with a partial insertion of two objects inside the cavity and displace them forth or back to "perturb" the fields. The mentioned region is limited by two asymptotical lines where the volume of the perturbing objects grow dramatically. At these points the perturbing objects are ineffective. On the other hand we notice that there exists a point at r/a=0.7 where the insertion of the only volume τ_2 is sufficient to fulfill both conditions on frequency shifts. At this point, in fact, the volume τ_2 subtracts the same amount of electric and magnetic energy for the fundamental mode, therefore affecting only the parasitic mode under investigation.

The point at r/a=0.5 (chosen in the region where both τ_1 and τ_2 are positive) of the above theoretical curve has been tested experimentally. In Fig. 3 the lower curve displays the unperturbed TM_{110} resonant spectrum. Being the real cavity not perfectly cylindrical, the mode degeneracy is removed and the spectrum exhibits two peaks at slightly different frequencies. The upper curve represents the "shifted" spectrum of the perturbed mode. The perturbation acts on the right peak for which we observe a shift of 87 kHz, in good agreement with the computed value of 95 kHz. It is worth noting that there is a perturbation also on the orthogonal mode. Smearing of resonant curves are due to bad RF contacts between perturbing objects and cavity walls. No shift has been observed for the fundamental mode.

The same mode has been investigated considering the $\phi = 0$ polarity. Condition on the HOM frequency shift yields:

$$\frac{\tau_2}{V\delta} = \frac{2}{3} \frac{\left(\frac{x_{11} r}{a}\right)^2 J_0^2(x_{11})}{J_1^2\left(\frac{x_{11} r}{a}\right)}$$

The theoretical curves of the normalized volumes are shown in Fig.4.

Also for this mode we have tested the point r/a=0.5. The measured frequency shift is 91 kHz, to be compared with the same value of 95 kHz, as found for $\phi = 0$. In this case the excitation and probe antennas were rotated by 90°. Results are shown in Fig. 5. We notice that also for this mode the insertion of a perturbing object τ_2 at r/a=0.7 alone satisfies the conditions on the frequency shifts.

A systematic analysis has been done theoretically for the first 10 modes. Here below we show some results for those modes tested also experimentally.

Mode TM_{011}.

The condition on the frequency shift yields:

$$\frac{\tau_2}{V\delta} = \frac{-J_1^2(x_{01})}{6\left(1+\frac{\lambda^2}{2d^2}\right)\left[J_0^2\left(\frac{x_{01}r}{a}\right) - \frac{1}{2}J_1^2\left(\frac{x_{01}r}{a}\right)\right]}$$

The behaviour of the normalized volumes τ_1 and τ_2 per unit of frequency shift versus r/a is shown in Figs.6 for δ=0.001.

For a given value of τ_1, (τ_2/V) is slowly increasing until r/a $\approx$ 0.6 and diverges for r/a $\rightarrow$ 0.7; for a given value of τ_2, on the contrary, (τ_1/V) is independent on r/a. For a theoretical Δf = 100 kHz, the corresponding measured value was 126 kHz (Fig. 7).

Mode TE_{011}

The condition on the HOM frequency shift yields:

$$\frac{\tau_2}{V\delta} = \frac{J_1^2(x'_{01}) - J_0(x'_{01})\,J_2(x'_{01})}{3\left\{\frac{\lambda^2}{4d^2}J_0'^2\left(\frac{x'_{01}r}{a}\right) + \frac{J_0^2(x'_{01})}{J_1^2(x_{01})}\left[2J_0^2\left(\frac{x_{01}r}{a}\right) - J_1^2\left(\frac{x_{01}r}{a}\right)\right]\right\}}$$

The behaviour of the normalized volumes τ_1 and τ_2 for a frequency shift δ=0.001 versus r/a is shown in Figs. 8.

Again, for a given value of τ_1, (τ_2/V) is slowly increasing until r/a $\approx$ 0.6 and diverges positively for r/a $\rightarrow$ 0.7; for a given value of τ_2, on the contrary, (τ_1/V) is greater than zero and slightly decreases until at r/a = 0.6 it becomes negative and diverges rapidly for r/a $\rightarrow$ 0.7. When (τ_1/V) crosses the zero-value the volume τ_2 only is sufficient. For a theoretical Δf = 125 kHz, the corresponding measured value was 145 kHz (Fig.9).

Mode TE_{111}

The condition on the HOM frequency shift yields ($\phi = \pi/2$):

$$\frac{\tau_2}{V\delta} = \frac{\frac{1}{2}J_0^2(x'_{11}) + J_1^2(x'_{11})\left(\frac{1}{2} - \frac{1}{x'^2_{11}}\right)}{3\left\{\frac{\lambda^2}{4d^2}J_1'^2\left(\frac{x'_{11}r}{a}\right) + \frac{J_1^2(x'_{11})}{J_1^2(x_{01})}\left[2J_0^2\left(\frac{x_{01}r}{a}\right) - J_1^2\left(\frac{x_{01}r}{a}\right)\right]\right\}}$$

The perturbing hemispheres are located in the same place as above, thereby producing a frequency shift of 93 kHz. The measured one is 109.5 kHz (Fig.10). Fig.11 shows again the behaviour of the frequency shift as function of r/a.

For the 90° rotated mode (ϕ = 0) we get:

$$\frac{\tau_2}{V\,\delta} = \frac{\frac{1}{2} J_0^2\left(x'_{11}\right) + J_1^2\left(x'_{11}\right)\left(\frac{1}{2} - \frac{1}{x'^{\,2}_{11}}\right)}{3\left\{\frac{\lambda^2 J_1'^2\left(\frac{x'_{11} r}{a}\right)}{4d^2 \left(\frac{x'_{11} r}{a}\right)^2} - 2\left[\frac{J_1\left(x'_{11}\right)}{x'_{11} J_1\left(x_{01}\right)}\right]^2 \left[2 J_0^2\left(\frac{x_{01} r}{a}\right) - J_1^2\left(\frac{x_{01} r}{a}\right)\right]\right\}}$$

Plots of (τ_1/V) and (τ_2/V) are shown in Figs. 12 It is worth noting that also in this case τ_1 is zero when τ_2 is located at a position r/a = 0.7. The measured frequency shift in this last case is 115 kHz (Fig.13) to be compared to 93 kHz.

4. - APPLICATION TO DAΦNE

DAΦNE is envisaged to operate with 120 bunches [3].There are 120 relative coupled-bunch modes with a relative phase shift

$$\Delta\phi = s\,(2\pi/120)\ ,\ s=0,1,.....119.$$

These modes have line frequencies at

$$\omega_{p,a,s} = (120p + s + a\nu_s)\,\omega_o\ ,\ p = 0, \pm 1, \pm 2,$$

where a indicates the phase space synchrotron motion mode: a=1 dipole, a=2 quadrupole etc. We have the synchrotron sidebands around a comb-like spectrum with ω_o = 20 Mrad/s spacing. In spite of a low coupling probability, a HOM can undergo a significant frequency drift, for example due to thermal effects, so that a sideband might be even fully coupled to a HOM giving rise to extreme and unmanageable growth rates of instabilities.Therefore a first very important requirement is on the thermal stabilization of the RF cavity. In order to limit the growth rates below reasonable values that can be counteracted by a feedback system, we are investigating two cures: Damping of HOM's, Tight control of HOM frequencies.

To illustrate the potentiality of the HOM shifting method, we report on some calculations, that have been made by means of the computer code ZAP [7] using the HOM spectrum of a preliminary cavity [8]. A list of 20 first longitudinal HOM's as found by the program URMEL [9] is shown in table I. We used this spectrum as input to ZAP, with the relevant DAΦNE parameters, and we evaluated the 5 coupled-bunch modes with the highest growth rates, which are listed in Table II for a=1 (dipole modes). The coupled-bunch mode s=91 at ω_p=6567 Mrad/sec is found to be the most unstable, although the shunt impedance of the corresponding parasitic mode J=8 source of the instability excitation, is not the highest in Table I.

Indeed, if we rerun ZAP assuming a damping factor 100 for the above cavity mode, we obtain a modest decrease of the growth rate for the relative mode s=91 (by only a factor 6), while the nearest modes s=90 and s=92 couple to a broader resonance and become strongly excited (Table III). On the contrary, assuming just a frequency shift by 1‰ and no damping at

all, the coupled-bunch mode s=91 disappears completely from the top list of the most dangerous relative modes (table IV).

In conclusion the frequency shift method has the very appealing feature of decoupling an unstable relative mode from the exciting parasitic cavity mode. However, the real feasibility of a frequency shift system relying upon this technique has still to be investigated. Furthermore, this technique could be used in combination with the damping technique, acting on those undamped modes with a growth rate too high to be cured by a feedback system.

5. - CONCLUSIONS AND FUTURE DEVELOPMENTS

The perturbation technique seems effective, at least in principle, in shifting the HOM frequencies of a RF cavity. The work presented in this paper is concerned with the HOM shifting of a pill box cavity. It has been possible to draw useful information about the general behaviour of the parasitic modes under the "perturbation" effect, and a first classification of modes has been done. A similar detailed analysis on a real cavity is now in progress to assess the full potentiality of the method. In particular is worth studying the effectiveness of the method combined with HOM damping techniques. The use of more objects to include the "tuning" of the fundamental mode and to control more HOMs is also in the aim of further studies.

ACKNOWLEDGEMENTS

The authors wish to thank Prof. Giorgio Gerosa, from the University of Rome, for many fruitful discussions and continuous encouragement.

REFERENCES

[1] Proposal for a Φ-Factory, LNF - 90/031 (R).

[2] See for instance: Y. Funakoshi et al., "Asymmetric B-Factory Project at KEK", Proceedings of the Workshop on Beam Dynamics Issues of High-Luminosity Asymmetric Collider Rings, Feb. 12-16, 1990, LBL, USA.

[3] DAΦNE Design Book (in prep.).

[4] G.Conciauro and P.Arcioni, "A new HOM-free Accelerating Resonator", Proc. of 2nd European Particle Accelerators Conference, Nice, June 12-16 1990, p.149.

[5] R.B.Palmer, "Damped Accelerator Cavities," SLAC-PUB-4542 (1988).

[6] L.C. Maier and J.C. Slater,"Field Strength Measurements in Resonant Cavities", J. of Appl. Physics, Vol.23, N. 1, (1962).

[7] M.S. Zisman, S. Chattopadhyay and J.J. Bisognano, "ZAP User's Manual", LBL 21270 (1986).

[8] S. Bartalucci, L. Palumbo and B. Spataro, "A Low Loss Cavity for DAΦNE", (DAΦNE Int. Note in prep.).

[9] T. Weiland, "On the Computation of Resonant Modes in Cylindrically Symmetric Cavities", Nucl. Instr. and Meth., Vol. 216, 329 (1983).

TABLE I - Monopole modes as computed by URMEL.

J	ωr (MRad/s)	Rs (MOhm)	Q
1	4595.0	0.300	63453
2	4730.0	0.150	75690
3	5562.0	0.002	72534
4	5582.0	0.325	53645
5	5702.0	0.013	70812
6	6907.0	0.032	74947
7	6453.0	0.097	72810
8	6563.0	0.076	62940*
9	7579.0	0.001	65987
10	8031.0	0.197	70436
11	8673.0	0.037	65085
12	9134.0	0.005	68371
13	9392.0	0.002	62976
14	9889.0	0.053	68371
15	9924.0	0.083	103612
16	10496.0	0.030	68437
17	10653.0	0.019	77311
18	10995.0	0.032	124888
19	11051.0	0.089	69119
20	11462.0	0.078	66477

TABLE II - The most dangerous coupled-bunch modes as computed by ZAP.

S	Freq. shift (1/s)	Growth rate(1/s)
91	-1.2028E+05	3.4395E+04
45	1.3738E+05	1.3878E+04
98	2.9080E+04	1.5747E+03
112	-6.1687E+03	8.3106E+01
77	1.1399E+04	7.1021E+01

TABLE III - As in Table II with a damping factor 100 applied on the mode J=8

S	Freq. shift (1/s)	Growth rate(1/s)
45	1.3738E+05	1.3877E+04
91	5.9146E+03	5.2447E+03*
98	2.9069E+04	1.5820E+03
90	7.3758E+03	3.4555E+02
92	4.8485E+03	3.35471E+02

TABLE IV - As in Table II with a 1‰ shift applied on the mode J=8.

S	Freq. shift (1/s)	Growth rate(1/s)
45	1.3738E+05	1.3878E+04
98	2.9090E+04	1.5747E+03
112	-6.1671E+03	8.3105E+01
77	1.1401E+04	7.1022E+01
19	1.8755E+03	5.3145E+01

APPENDIX I : FIELDS OF A PILL BOXCAVITY

Mode TM_{010} (fundamental mode : f=356.3781 MHz)

The fields components are:

$$E_z(r) = E_o\, J_o\left(\frac{x_{01}\, r}{a}\right) \qquad H_\phi(z) = j\,\frac{E_o}{Z_o}\; J_1\left(\frac{x_{01}\, r}{a}\right)$$

where x_{01} is the first zero of the Bessel function $J_0(x)$, and Z_0 is the vacuum impedance (120π Ω).

Mode TM_{110} (f=566.6412 MHz)

The field components are:

$$E_z(r,z) = E_0\, J_1\left(\frac{x_{11}\, r}{a}\right) \sin(\phi)$$

$$H_r(r,z) = j\,\frac{E_0}{Z_0}\left(\frac{a}{x_{11} r}\right) J_1\left(\frac{x_{11}\, r}{a}\right)\cos(\phi) \qquad H_\phi(r,z) = -j\,\frac{E_0}{Z_0}\; J_1'\left(\frac{x_{11}\, r}{a}\right)\sin(\phi)$$

with $J_1(x_{11})=0$.

Mode TM_{011} (f = 580.8963 MHz)

The fields components are:

$$E_r(z,r) = E_0\left(\frac{\lambda}{2d}\right) J_1\left(\frac{x_{01}\, r}{a}\right)\sin\left(\frac{\pi}{d}\, z\right) \qquad E_z(z,r) = E_0\; J_0\left(\frac{x_{01}\, r}{a}\right)\cos\left(\frac{\pi}{d}\, z\right)$$

$$H_\phi(z,r) = -j\,\frac{E_0}{Z_0}\; J_1\left(\frac{x_{01}\, r}{a}\right)\cos\left(\frac{\pi}{d}\, z\right)$$

where λ=c/f.

Mode TE_{011} (f = 730.5751 MHz)

The field components are:

$$E_\phi(r,z) = j\; E_0\; J_0'\left(\frac{x_{01}'\, r}{a}\right)\sin\left(\frac{\pi\, z}{d}\right)$$

$$H_r(r,z) = \frac{E_0}{Z_0}\left(\frac{\lambda}{2d}\right) J_0'\left(\frac{x_{01}'\, r}{a}\right)\cos\left(\frac{\pi\, z}{d}\right) \qquad H_z(r,z) = \frac{E_0}{Z_0}\; J_0'\left(\frac{x_{01}\, r}{a}\right)\sin\left(\frac{\pi\, z}{d}\right)$$

Mode TE_{111} (f = 534.5671 MHz)

The fields components are:

$$E_r(r,\phi,z) = -j\,E_0\left(\frac{a}{x'_{11}r}\right) J_1\left(\frac{x'_{11}r}{a}\right)\cos(\phi)\sin\left(\frac{\pi z}{d}\right)$$

$$E_\phi(r,\phi,z) = j\,E_0\; J'_1\left(\frac{x'_{11}r}{a}\right)\sin(\phi)\;\sin\left(\frac{\pi z}{d}\right)$$

$$H_r(r,\phi,z) = \frac{E_0}{Z_0}\left(\frac{\lambda}{2d}\right) J'_1\left(\frac{x'_{11}r}{a}\right)\sin(\phi)\;\cos\left(\frac{\pi z}{d}\right)$$

$$H_z(r,\phi,z) = \frac{E_0}{Z_0}\; J_1\left(\frac{x'_{11}r}{a}\right)\sin(\phi)\;\sin\left(\frac{\pi z}{d}\right)$$

$$H_\phi(r,\phi,z) = \frac{E_0}{Z_0}\left(\frac{\lambda}{2d}\right)\left(\frac{a}{x'_{11}r}\right) J_1\left(\frac{x'_{11}r}{a}\right)\cos(\phi)\;\cos\left(\frac{\pi z}{d}\right)$$

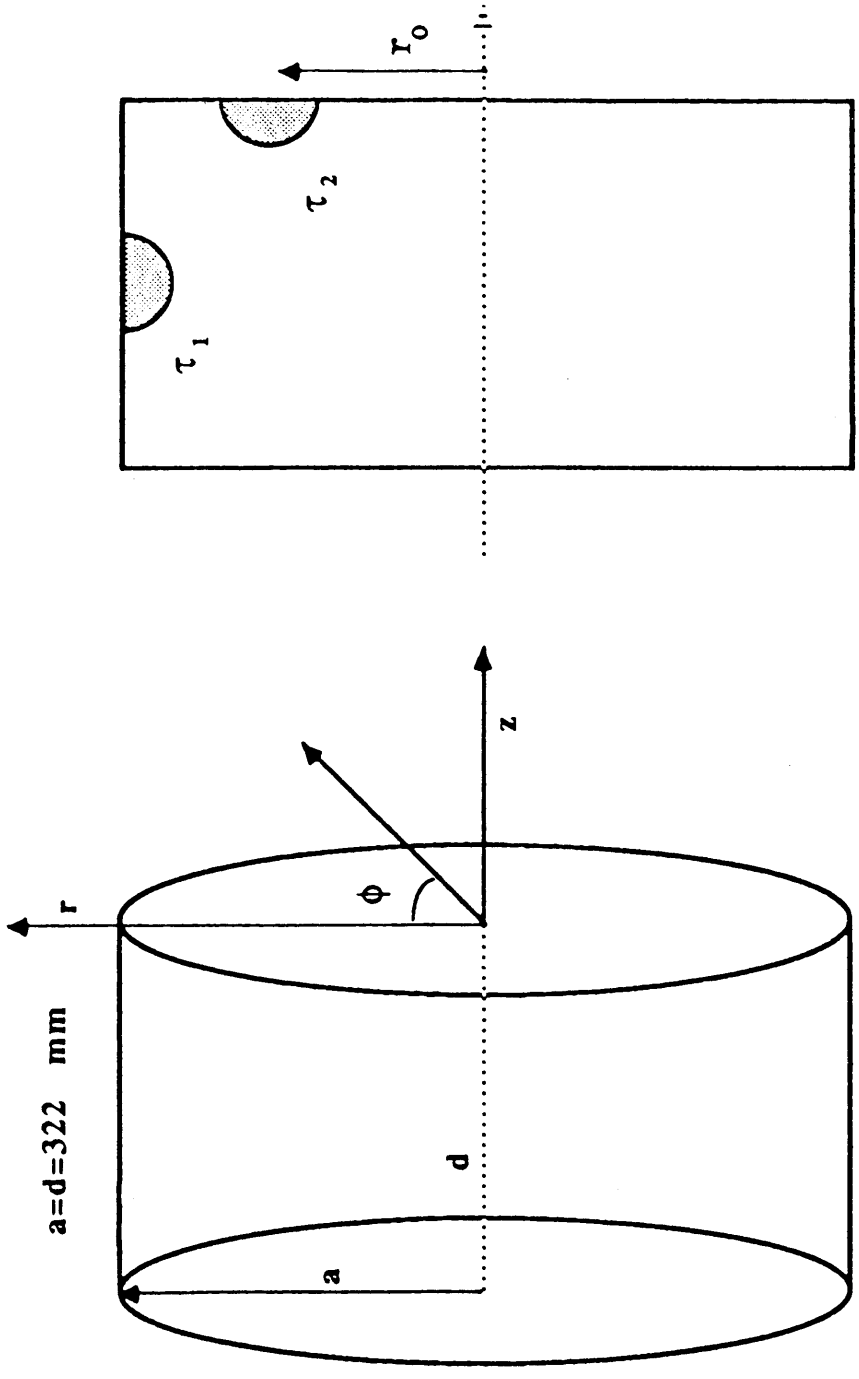

Fig.1

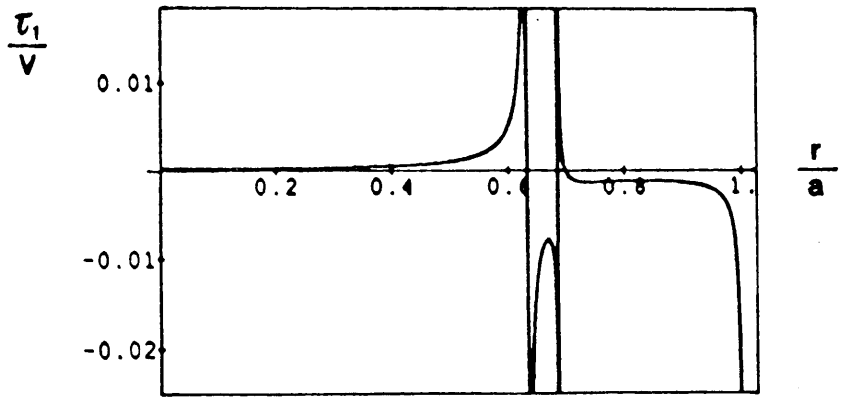

FIG. 2a

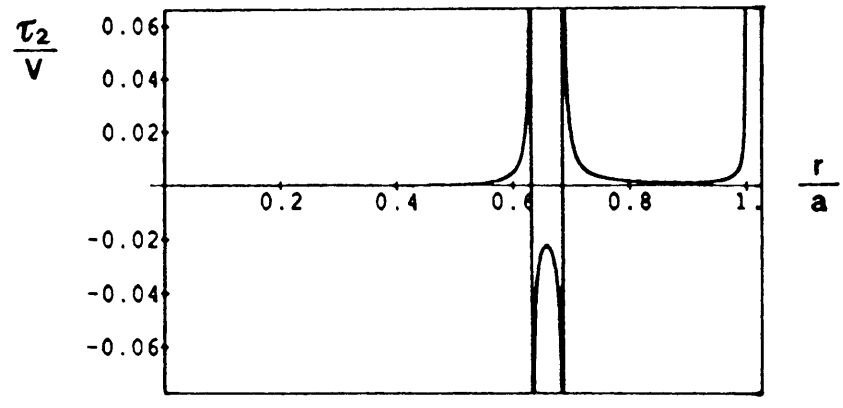

FIG. 2b

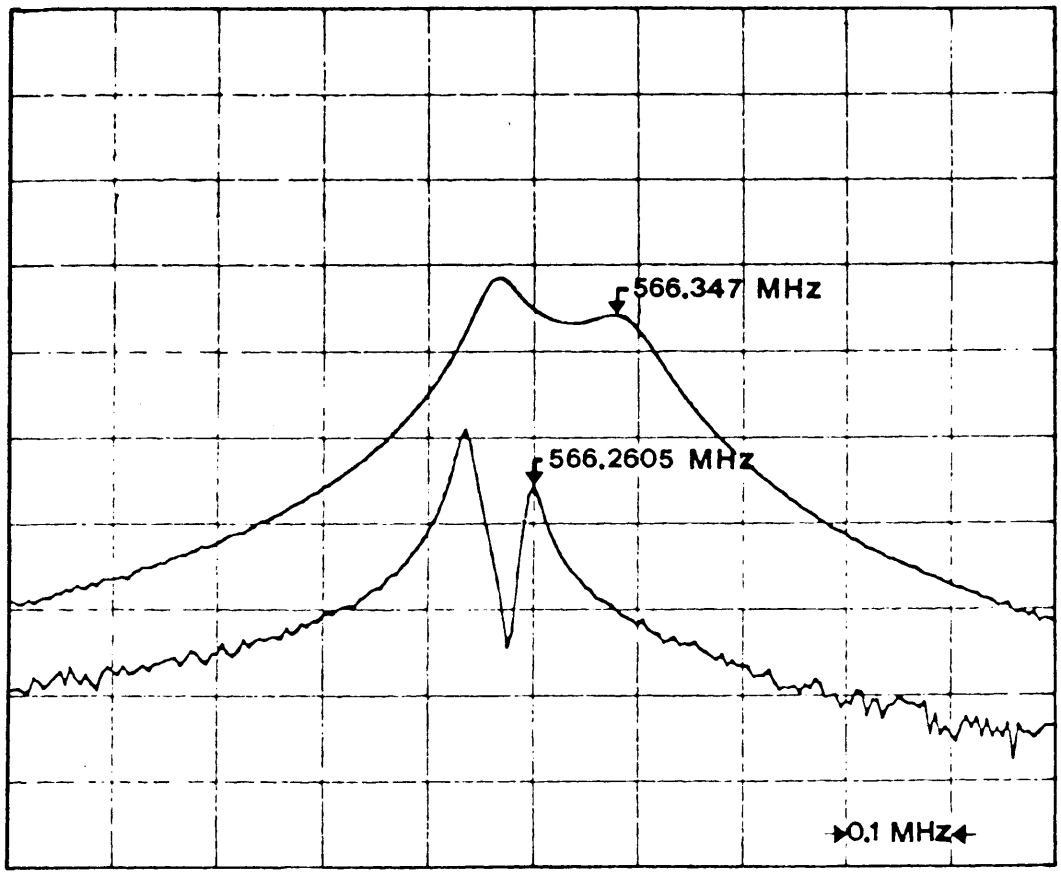

FIG. 3

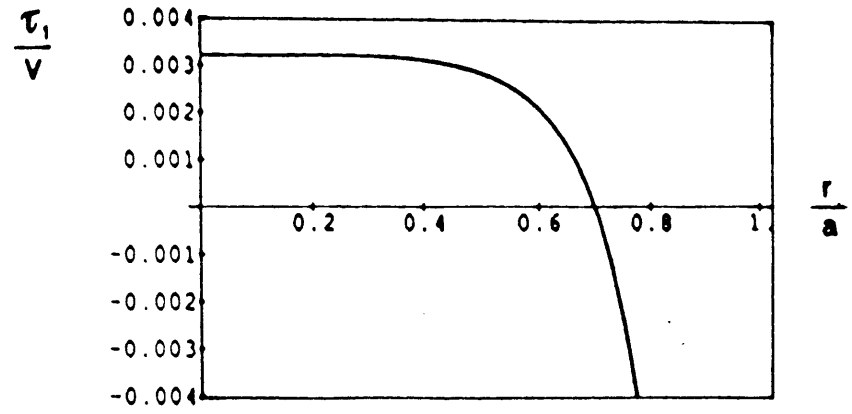

FIG. 4a

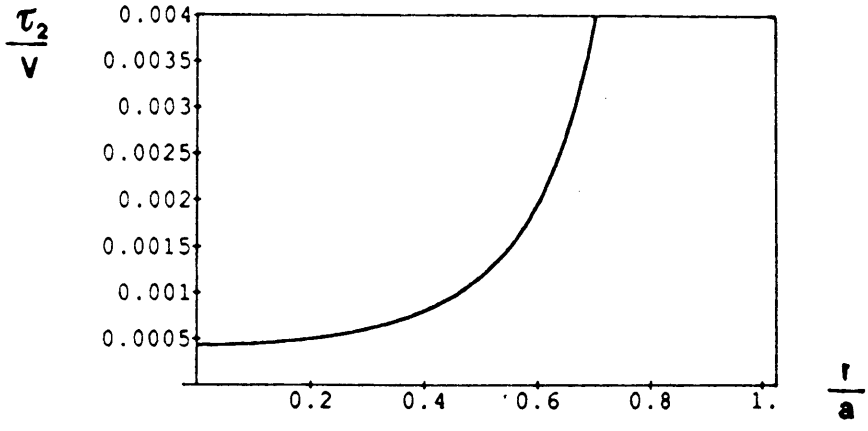

FIG. 4b

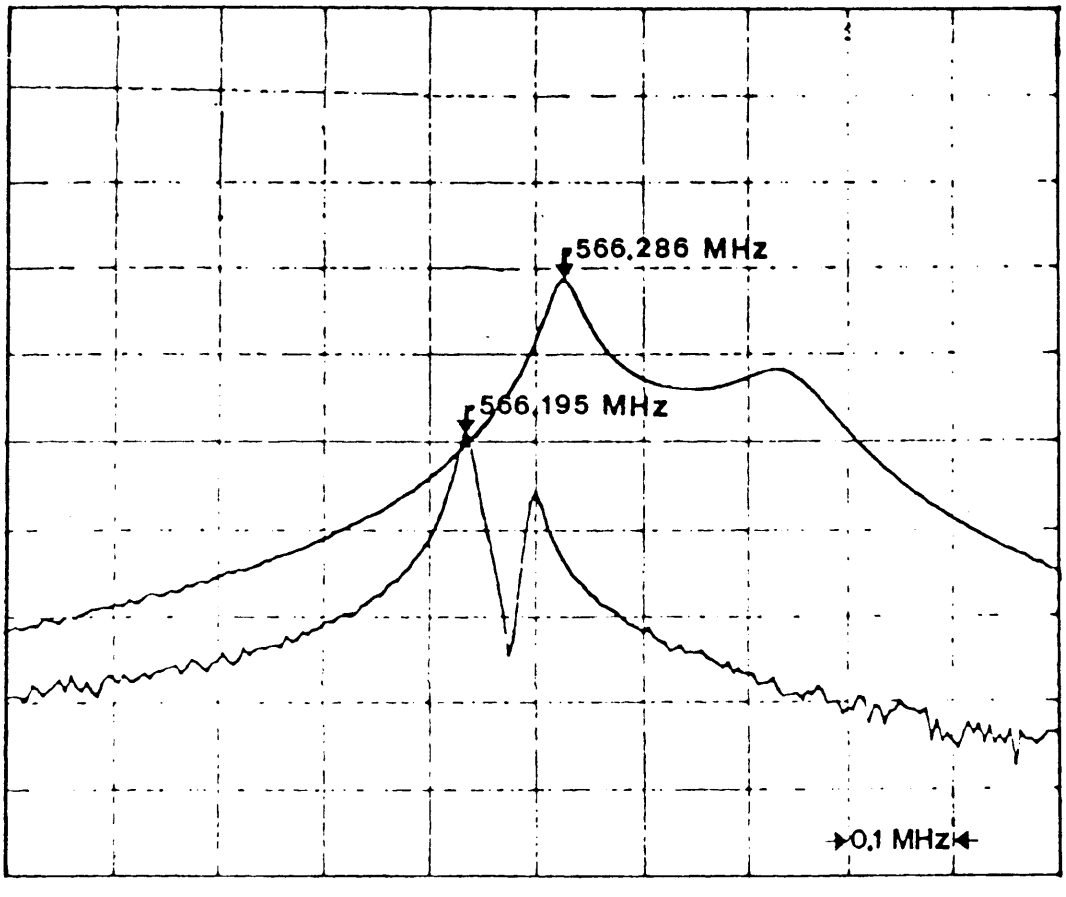

FIG. 5

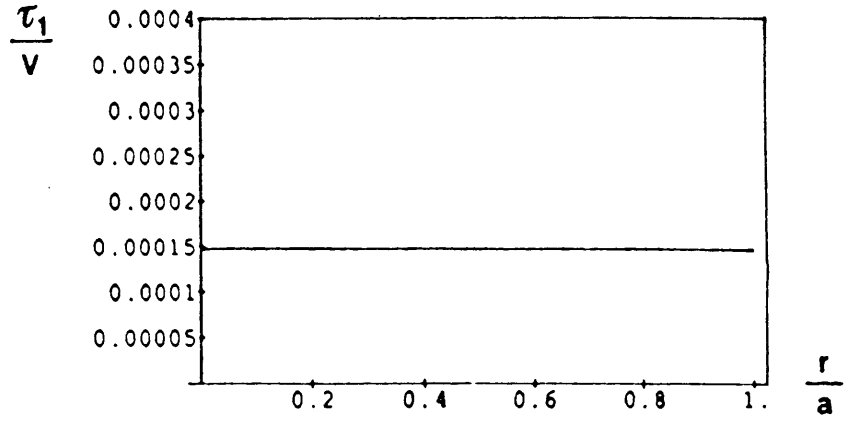

FIG. 6a

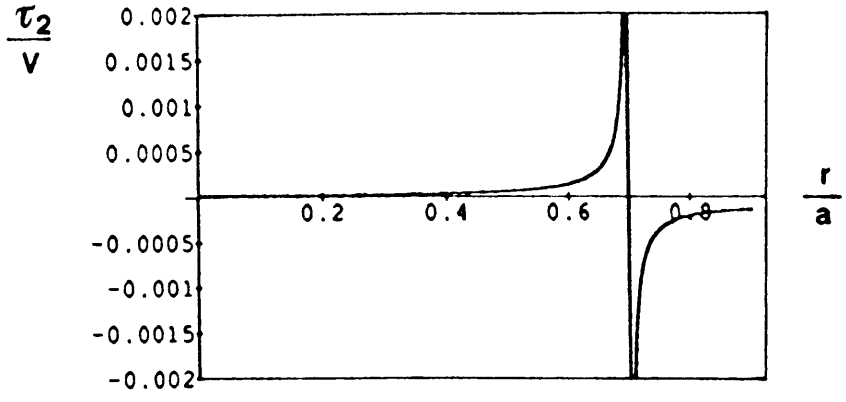

FIG. 6b

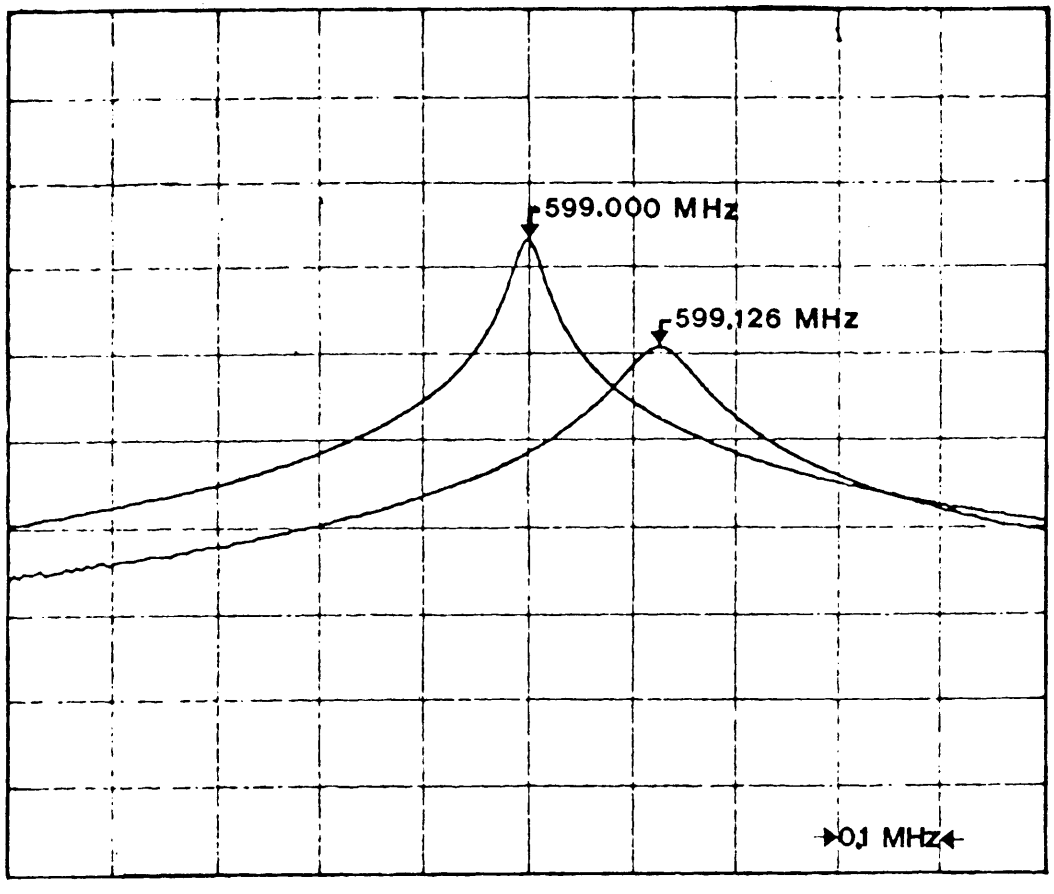

FIG. 7

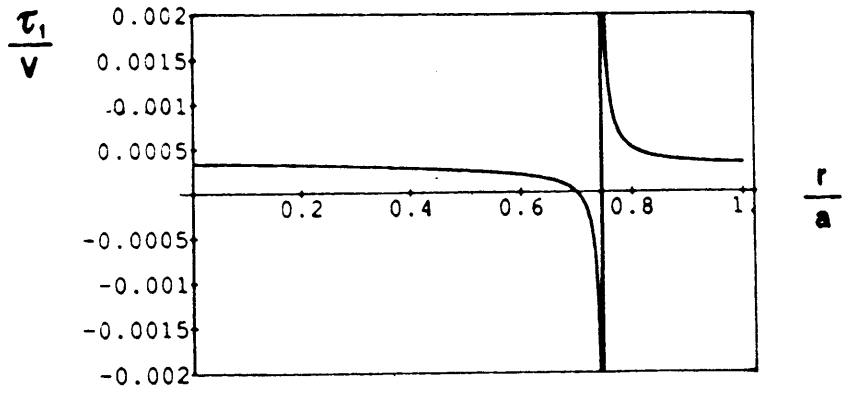

FIG. 8a

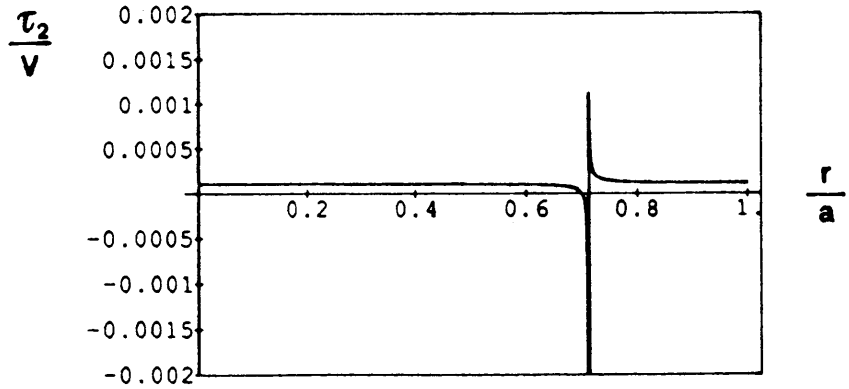

FIG. 8b

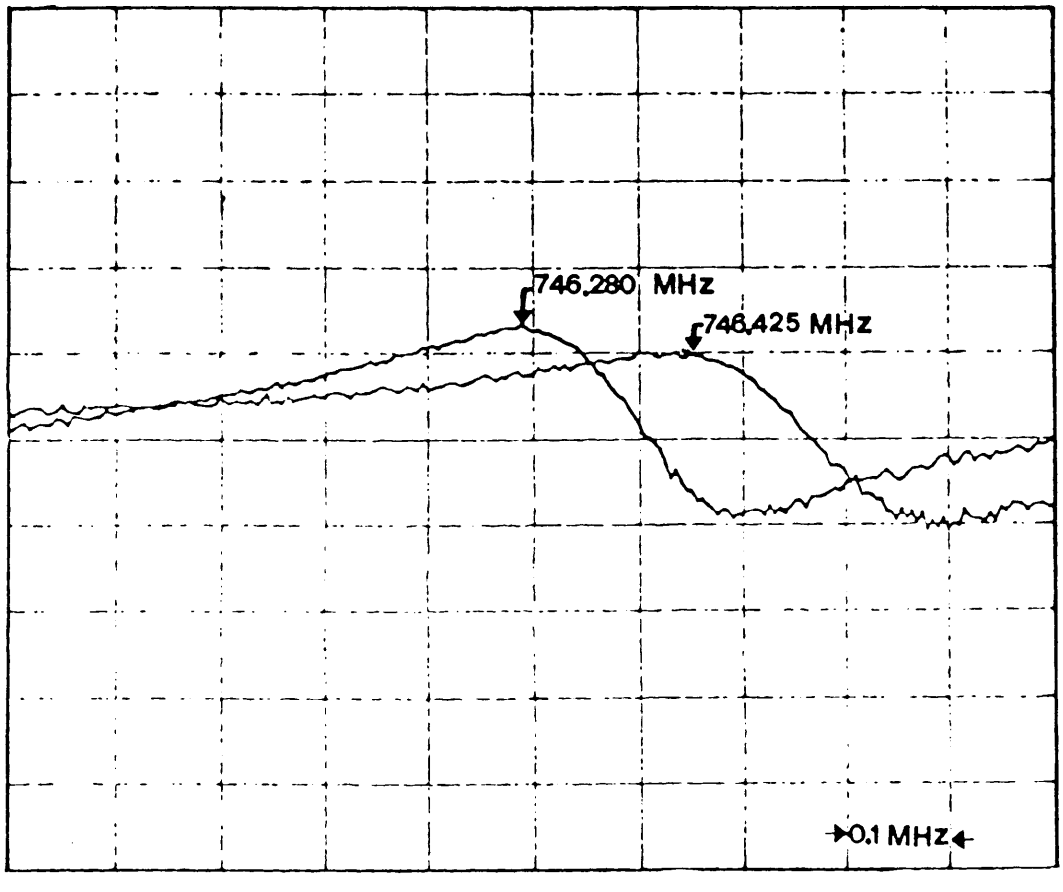

FIG. 9

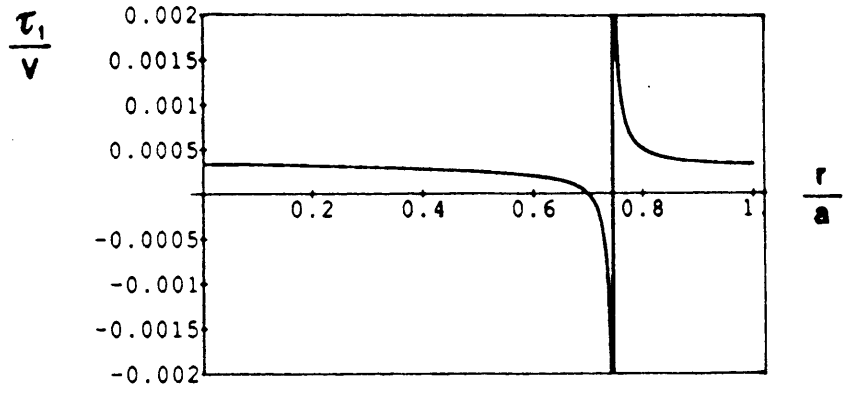

FIG. 10a

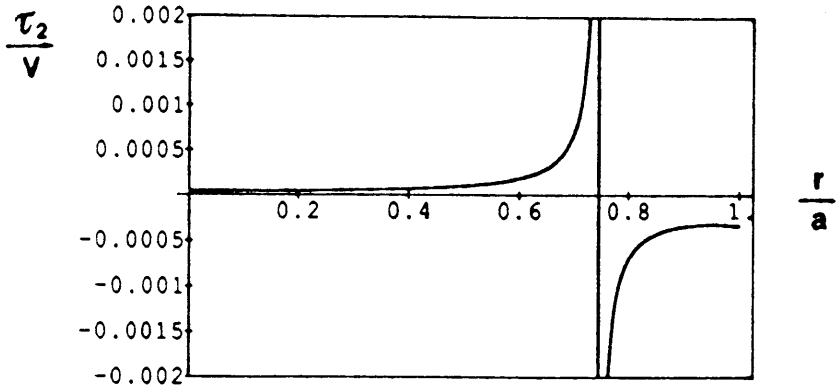

FIG. 10b

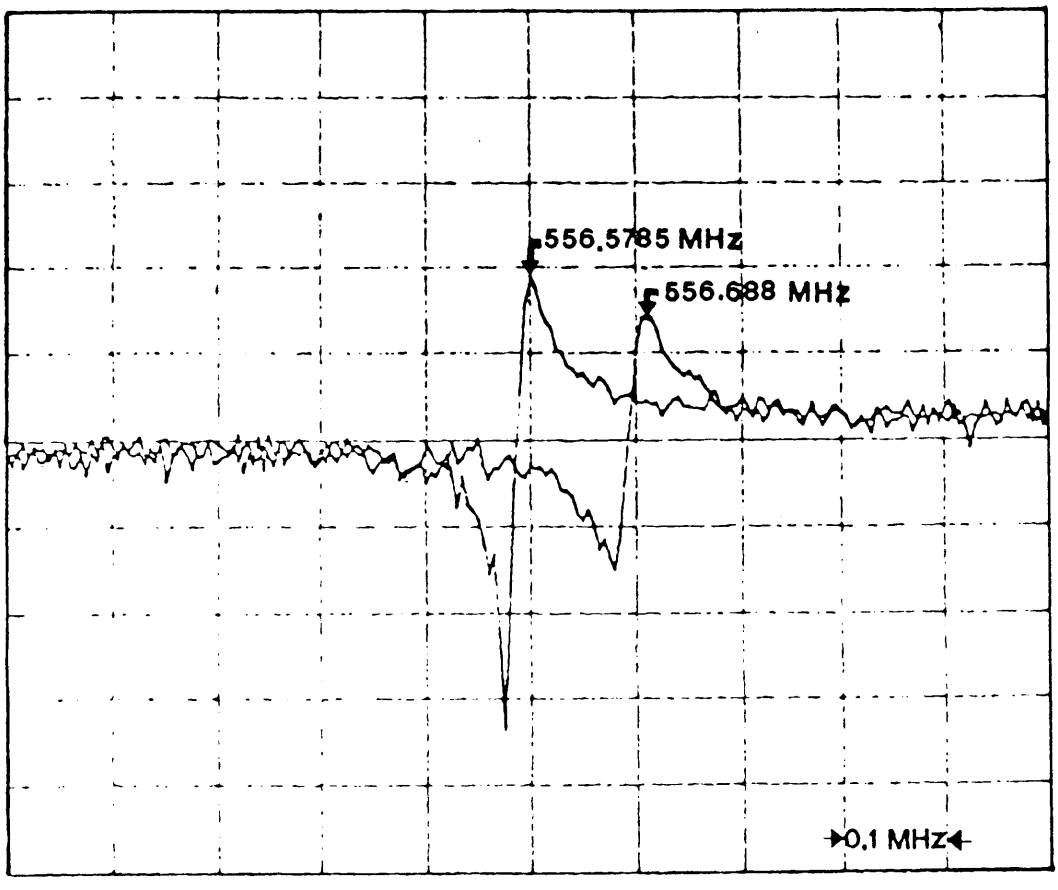

FIG. 11

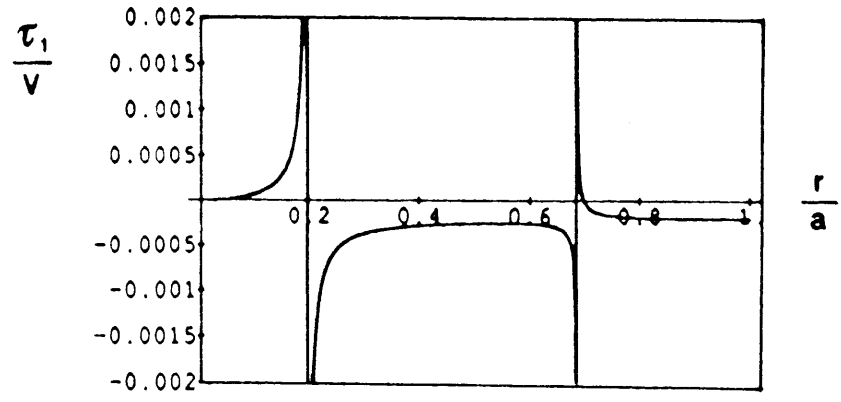

FIG.12 a

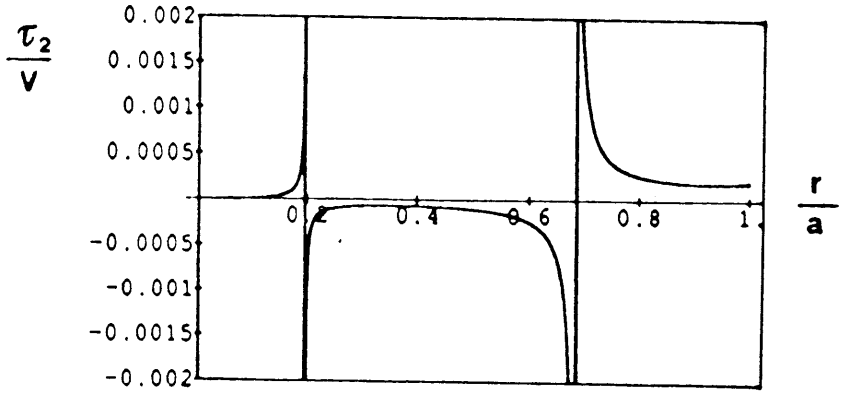

FIG.12b

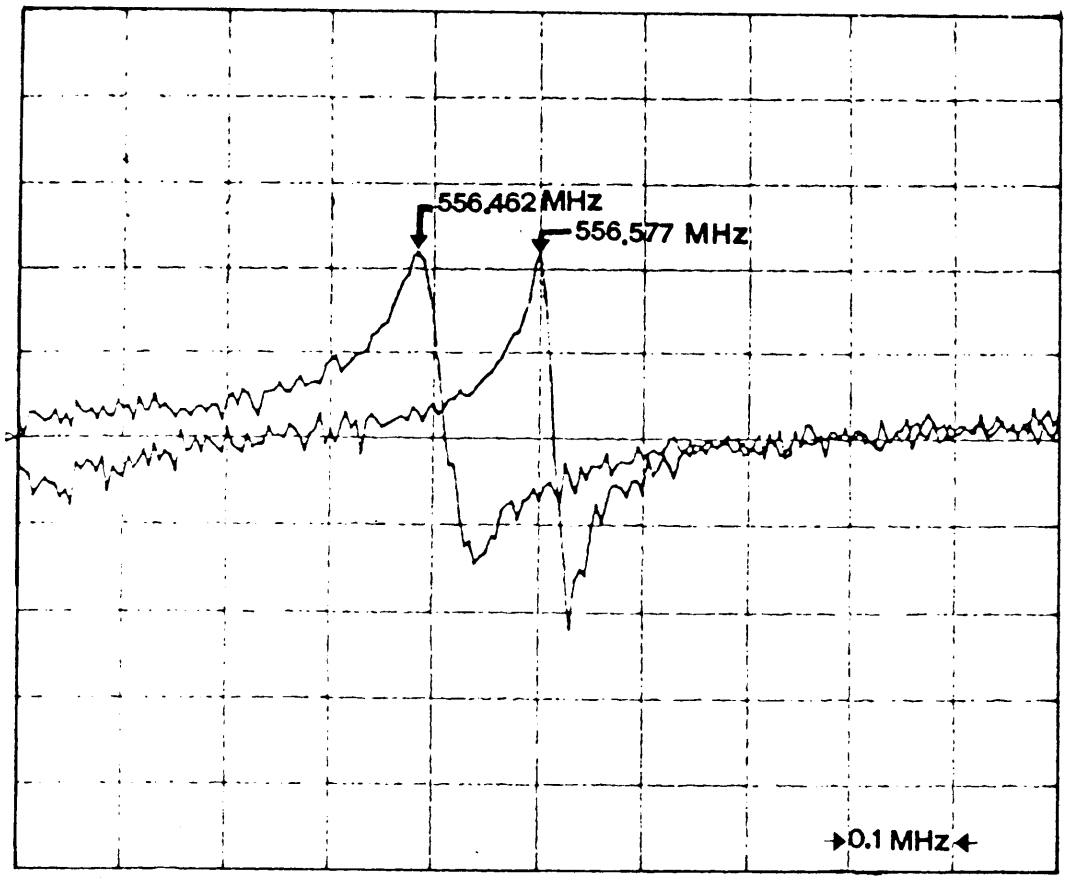

FIG.13